

Supplementary Information

Efficacy of tyrosine kinase inhibitors by a combination of Raman micro-spectroscopy and deep wavelet scattering-based multivariate analysis framework

Irina Schuler,^{a,b} Martin Schuler,^{a,b} Tatjana Frick,^{a,b} Dairovys Jimenez,^{a,b} Abdelouahid Maghnouj,^c Stephan Hahn,^c Rami Zewail,^d Klaus Gerwert,^{a,b} and Samir F. El-Mashtoly^{*a,b,e,†}

^aCenter for Protein Diagnostics (PRODI), Ruhr-University Bochum, Bochum, Germany

^bDepartment of Biophysics, Ruhr-University Bochum, Bochum, Germany

^cDepartment of Molecular GI-Oncology, Clinical Research Center, Ruhr-University Bochum, Bochum, Germany

^dDepartment of Computer Science & Engineering, Egypt-Japan University of Science & Technology, New Borg El-Arab, Egypt

^eBiotechnology Program, Institute of Basic and Applied Science, Egypt-Japan University of Science & Technology, Alexandria, Egypt

*Samir.Elmashtoly@leibniz-ipht.de

Experimental Section

Cell Viability Assay

For the MTT viability assay, 10,000 SK-BR-3 cells per well in 100 μ l of complete DMEM were incubated in a 96-well plate for 24 h at 37 °C and 5 % CO₂ atmosphere. Then, 100 μ l of DMEM was added containing different concentrations of the drugs lapatinib and neratinib (0.1, 0.5, 1, 5, 20, 50 μ M). Cells were incubated for a further 16 h. Afterward, 50 μ l of MTT-solution was added to each well and the solution was then incubated for 2 h in the incubator at 37 °C. The media and MTT were sucked away, and the cells were resuspended in 200 μ l of DMSO. To dissolve the formazan crystals, the plate was placed on a shaker for 15 minutes. At last, the absorbance was measured at 550 nm (purple formazan) and the reference was taken at 620 nm (yellow MM) on the microplate reader (TECAN Sunrise, Austria). Four replicates are used for each concentration. The cell viability in each sample was normalized to that of the control sample.

Real-time cell analysis (RTCA)

Cells were prepared according to the splitting protocol. Then, the cells are counted with the Neubauer chamber and diluted to the final concentration of 10,000 cells/100 μ l. During the splitting, 100 μ l of DMEM was added to the microtiter plate to equilibrate the electrodes for 20 min. After that, the cells were added to the wells and the plate was not moved for 30 min to let the cells settle. The RTCA was performed using the xCELLigence DP system (Bioscience) where the plate is placed after the equilibration time. The cells were incubated for 24 h, at 37 °C in the system. Subsequently, the drugs were added in the same concentrations as in the MTT assay in 50 μ l complete DMEM. The cells were monitored for 120 h after adding the drug.

Cell Cycle Analysis

Cells were prepared after the passage protocol and then seeded out in six-well plates with around 100,000 cells/well. When the wells reached a confluence of cells around 40 %, the same drugs, in the same concentration as used in the Raman measurements, were added in 5 ml of complete DMEM to the well and incubated for 24 h at 37 °C and 5 % CO₂ atmosphere. On the next day, cells were trypsinized, centrifuged, and counted. Around 200,000 cells per well were resuspended in 1 ml 1x PBS. Afterward, cells were centrifuged for 5 min at 17000 g and 4 °C, 900 μ l of the supernatant was discarded and the cell pellets were resuspended in the remaining 100 μ l. In addition, 500 μ l of ice-cold absolute methanol (fixation, dehydration of cells) was added and incubated for 1 h at -20 °C in the fridge. As propidium iodide (PI) binds not only to the dsDNA but also intercalates to double-stranded RNA, cells were treated with RNase to ensure only the DNA is bound to PI.¹ After the incubation time, the fixed cells were centrifuged for 10 min at 200 g at room temperature and the supernatant was discarded. 400 μ l of the PI staining solution was added per tube and incubated for 10 min without resuspending the cell at room temperature. Then, cells were resuspended and incubated light-protected for 60 min. At last, the cell suspensions were transferred to test tubes and vortexed to reach a single cell suspension, which was then measured in the FACSCanto™ II (BD Bioscience, FranklinLakes, US.).

Apoptosis Assay

Cells were prepared after the passage protocol in petri dishes. Cells were incubated at 37 °C and 5 % of the CO₂ atmosphere until the confluence reached 60-70 %. Then, the media was sucked away and fresh complete DMEM containing either just medium or lapatinib, or neratinib, each in the end concentration of 0.1 μM and 1 μM, was added to the dish, resulting in five prepared dishes including one control. The drugs were incubated for 16 h. After that, cells were passaged according to the splitting protocol and resuspended in 400 μl of 1x annexin buffer (10 mM HEPES, 140 mM NaCl, 2.5 mM CaCl₂, pH 7.4). Cells were counted with the Neubauer chamber and diluted with the 1x annexin buffer to 200,000 cells/200 μl in test tubes. In the end, each sample results in four tubes each containing 200 μl of the cell suspension. Tube 1 was without staining in comparison to the other tubes. Tube two was used to detect the phosphatidylserine, therefore 5 μl of the Annexin V was added. Tube three was used to dye the necrotic cells, therefore 2 μl of PI (100 μg/ml) was added. In tube four both substances were added. All tubes were incubated on ice in the dark for 15 minutes. At last, samples were analyzed by flow cytometry (FACSCanto™ II, BD Bioscience), where the emission was measured at 530 nm and >575 nm. During the measurement, cells were separated into different populations, dependent on whether cells were alive, apoptotic, or dead.

Immunofluorescence staining and fluorescence microscopy

Immunofluorescence was used to show the distribution of the tyrosine kinase receptors, EGFR and HER2, in the presence and in the absence of lapatinib and neratinib. Therefore, the SK-BR-3 cells were prepared on coverslips and permeabilized with 0.2 % Triton X100 for ten minutes. Next, the slides were washed three times for 5 min with 1x PBS. To reduce non-specific binding, all slides were incubated in a 1 % BSA/PBS solution for 30 min. Afterward, a primary antibody solution was prepared, which contains the EGFR targeting D28B1 rabbit mAb in the final concentration of 1:50 and the HER2 targeting CB mouse mAb with the final concentration of 1:1 in 1 % BSA/PBS. The slides were incubated with the primary antibody solution using the wet chamber principle at 4 °C overnight. Then, the slides were washed three times with PBS to remove unbound antibodies and incubated with the secondary antibody solution for one hour in the dark at 4 °C. The secondary antibody mix contains donkey-anti-rabbit TRITC and donkey-anti-mouse FITC in the final concentration of 1:100 in 1 % BSA/PBS. The secondary antibodies are coupled with a fluorophore. The slides were washed three times with PBS and incubated with DRAQ-5 in a concentration of 1:1000 in 1 % BSA/PBS for ten minutes.

After the staining, the fluorescence imaging was acquired using a confocal laser scanning microscope (Leica TCS SP5 II) with a Leica HCX PL APO (25x/ 1.4 NA) water immersion objective using three excitation wavelengths. The HER2 was excited at 488 nm, the EGFR excited at 561 nm and the DRAQ-5 excited at 633 nm. The measurement started with 561 nm and was continued with 488 nm to avoid strong photobleaching.

Correlative Raman and fluorescence imaging.

Raman imaging and fluorescence imaging were performed separately and sequentially on different instruments. Fluorescence staining was performed after the Raman measurements as described. To find the same cells measured by the Raman microscope under the fluorescence microscope, CaF₂ slides were first engraved in a checkerboard pattern with a diamond stylus tip before coating and growing cells on them. This allowed the localization of cells or cell clusters region by region, even with different microscope orientations (upright vs. inverted). In addition, white light overview images of the entire slide were taken before Raman measurement of specific cells to facilitate localization of cells using the same WITec confocal upright microscope used for Raman measurements. The microscope software (WITec Project Four) enabled precise automated labelling of cells measured by Raman scanning in the respective overview image.

Together with the engraved checkerboard pattern and the white light overview image with the labelled and measured cells, the previously measured cells could be localized after fluorescence staining and in the second microscope (Leica, SP5, inverted microscope) for fluorescence imaging. Fluorescence imaging was performed with the same pixel resolution as Raman microspectroscopic imaging to allow easy overlay of the images.

The overlay and alignment of Raman microspectroscopic filter images and fluorescence images (as shown in Figure 9) were performed manually in MATLAB 8.2 (MathWorks Inc., MA).

Western Blot

To gain the protein mixture, 100 µl of the cell suspension was passaged in six-well plates with 5 ml of complete DMEM in each well. Cells were incubated in 5 % CO₂ at 37 °C until they reached a confluence of 80 %. Afterward, lapatinib and neratinib were added in three different concentrations of 0.1, 0.5, and 1 µM and incubated for 16 h. After the incubation time, the media was removed, and the cells were washed three times with PBS. To each well, 250 µl of the lysis buffer, was added and the cells were scraped from the wells and collected in tubes. The lysis buffer is a mixture of RIPA (radioimmunoprecipitation assay) buffer with protease and phosphatase inhibitors. The mixture lyses the cell, prevents proteolytic degradation, and ensures the same phosphorylation state of the sample during protein extraction. In addition, ultrasonic lysis was used with a pulse mode of 10 sec on the cell suspension to guarantee that proteins of the membrane were released. The cell suspension was centrifuged for ten minutes at 4 °C at 13200 rpm (Eppendorf® Microcentrifuge 5415R, Hamburg, Germany), and the supernatant, which contains the proteins, was transferred to new Eppendorf tubes. Next, the protein concentration was measured against a BSA calibration curve in a Bradford protein concentration assay using a Nanodrop 2000c spectrophotometer (VWR Life Science, Erlangen, Germany). After that, the lysates were diluted with the lysis buffer to reach the same relative concentration in all the samples. 24 µl of each cell lysate were denatured for 5 min at 94 °C and then loaded with 5 µl of the prestained marker into the gel pockets of 10 % SDS-PAGE gels, which were prepared.

The separated proteins were transferred from the gel onto the nitrocellulose membranes using the BioRad Trans-Blot Semi-Dry transfer cell (BioRad Laboratories, Hercules, California) at a constant current of 300 mA for 30 min. Before the antibody incubation, the membranes are blocked with a 5 % BSA/milk (dependent on the antibody) in TBS-T solution for 1 h. The membranes are incubated with diluted antibodies against p/tAKT (60 kDa) and p/ERK 1/2 (44,42 kDa) separately, after the blocking, overnight at 4 °C. Then, the membranes were washed three times with TBS-T for ten minutes and next, incubated with the secondary horseradish peroxidase-conjugated antibodies to anti-rabbit (dilution 1:5000) and anti-mouse (dilution 1:2500) in 5 % BSA/milk TBS-T for one hour at 4 °C. In the last step, the membranes were washed two times with TBS-T and kept in TBS until the detection. To detect the proteins by chemiluminescence a ChemiDocMP (BioRad Laboratories, Hercules, California) was used for 10 min in the signal accumulation mode. Therefore, each membrane is covered in 1 ml of the SuperSignal West Pico Chemiluminescence Substrate (ThermoFisher) and placed in the detector.

Results and Discussion

Table S1. Control cells versus neratinib-treated cell classification using scattering-PCA framework with different dimensions for selected scattering subspace.

Scattering subspace dimension	F1-score	Accuracy
8-dimensional subspace	0.95	0.95
16- dimensional subspace	0.95	0.95
150- dimensional subspace	1	1
400-dimensional subspace	0.875	0.88

Table S2. Cell cycle analysis of SK-BR-3 cells. Cells were treated with different concentrations of lapatinib and neratinib. The cell number in different phases of the cell cycle is shown in percent.

	Concentrations of drugs in μM	G1 phase (%)	S phase (%)	G2/M phases (%)
Control		56.7	3.92	35.7
Neratinib	0.1	89.7	1.61	7.00
	0.5	81.9	1.53	16.3
	1.0	100	0	0
Lapatinib	0.1	95.6	1.04	2.99
	0.5	95.3	0.52	3.08
	1.0	100	0	0

During the cell cycle analysis, the total cellular DNA content of the prepared sample is analysed. The cell cycle can be analysed by using propidium iodide (PI), which binds to free nucleic acids in the cell as a red fluorescence dye for staining the DNA.² Afterward, flow cytometry is performed, and a histogram is generated. Flow cytometry was used to investigate the cytostatic effect of lapatinib and neratinib on the cells. This was evaluated by monitoring the percentages of a cell population in the different phases of the cell cycle. The phases of the untreated cells (control) are divided into 57 % of the cells in the G1-phase, 4 % in the S-phase, and 36 % in the G2/M-phases as shown in Table S2. This shows that at the time of the cell fixation around 36 % of cells are proliferating normally. Treatment of SK-BR-3 human breast cancer cells for 24 hours with different concentrations of lapatinib and neratinib (0.1-1.0 μM) resulted in a significant reduction in the G2/M phases and an increase in the G1 phase. For instance, almost all cells were arrested in the G1 phase (around 95 %) when cells were treated with 0.1 or 0.5 μM of lapatinib, whereas around 3% were in the G2/M phases. Cells treated with 0.1–0.5 μM neratinib displayed that around 80–90% of cells were in the G1 phase, while around 7–16% were in the G2/M phases. It is noted that the percentage of cell arrest upon treatment with neratinib does not increase with increasing concentration but is still significantly higher compared to the control group. On the other hand, cells treated with either 1 μM lapatinib or neratinib were completely arrested in the G1 phase.

The cell cycle assay demonstrates clearly that both drugs induce a cell cycle arrest in the G1 phase. The G1 phase is also considered a cell cycle checkpoint, which is controlled by internal (CDKs and pRb) factors. Cells can either pass the checkpoint and continue with the cell division or be moved to the non-dividing G0 phase.³ The RTCA and the cell cycle results show that the drugs have a cytostatic effect on the cancer cells in the first 24 hours. In addition, cells are stuck at the G1 restriction point of the cell cycle, underlining that cyclin D1 is probably downregulated and, therefore, the cells are located in a non-dividing state after binding the drugs.³

Table S3. Control cells versus lapatinib-treated cell classification.

Control vs lapatinib-treated cells (0.5 μM)			
Method	PCA	ICA	Scattering PCA
Precision	0.84848	1	1
Sensitivity	1	0.96429	1
Specifity	0.75	1	1
Accuracy	0.89583	0.97917	1
F1-score	0.91803	0.98182	1
Control vs lapatinib-treated cells (1 μM)			
Precision	1	1	1
Sensitivity	0.625	1	1
Specifity	1	1	1
Accuracy	0.89286	1	1
F1-score	0.76923	1	1

Table S4. Control cells versus neratinib-treated cell classification.

Control vs neratinib-treated cells (0.5 μM)			
Method	PCA	ICA	Scattering PCA
Precision	0.91429	0.9697	1
Sensitivity	1	1	0.96875
Specifity	0.85	0.95	1
Accuracy	0.94231	0.98077	0.98077
F1-score	0.95522	0.98462	0.98413
Control vs neratinib-treated cells (1 μM)			
Precision	0.82609	0.89474	0.90909
Sensitivity	0.95	0.85	1
Specifity	0.8	0.9	0.9
Accuracy	0.875	0.875	0.95
F1-score	0.88372	0.87179	0.95238

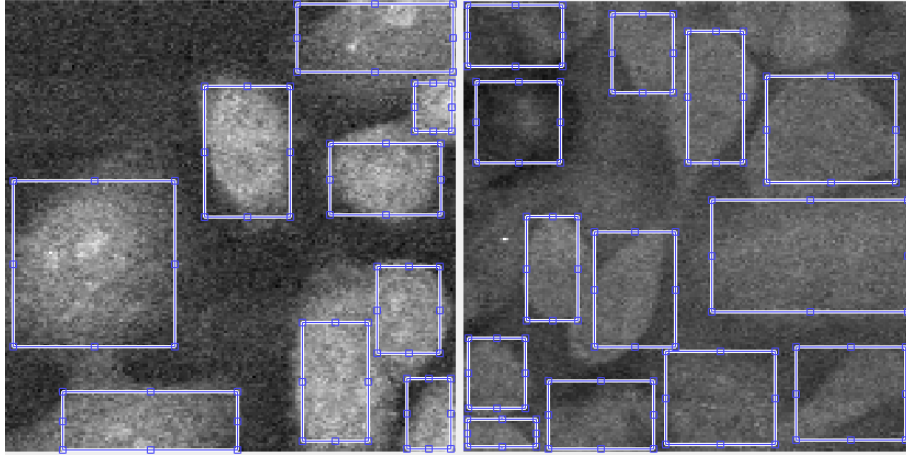


Figure S1. Example of the cell cropping process for (a) control (drug-free cells), (b) lapatinib-treated cells.

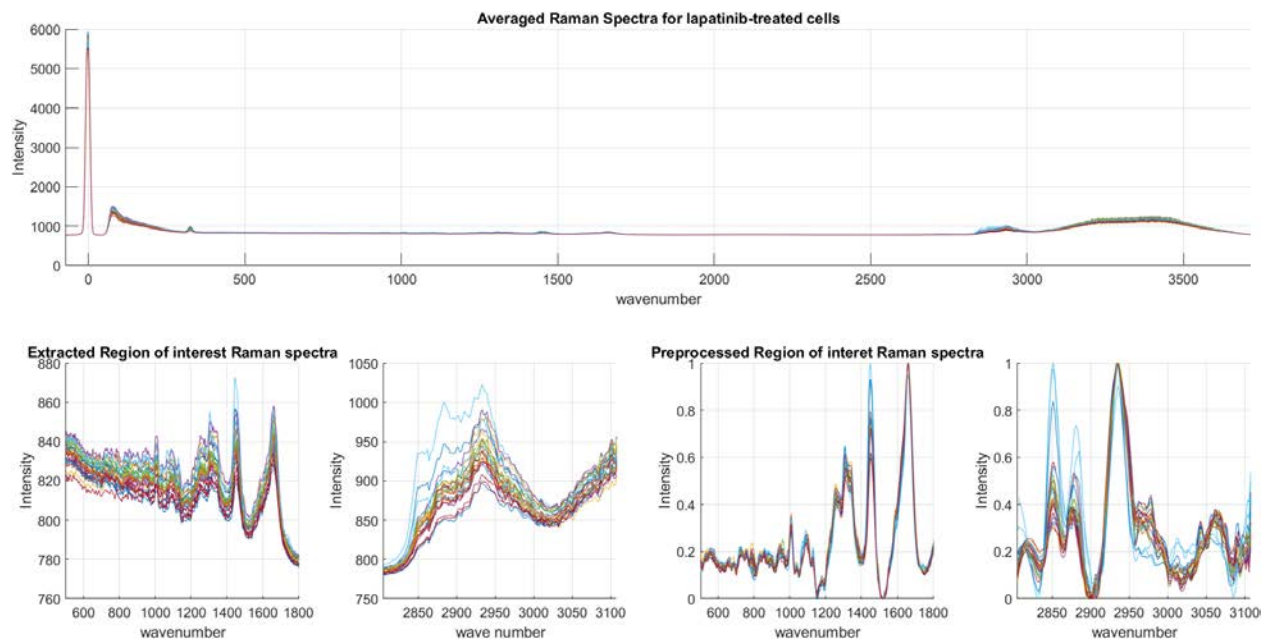


Figure S2. Example of preprocessing of the Raman spectra for lapatinib-treated cells.

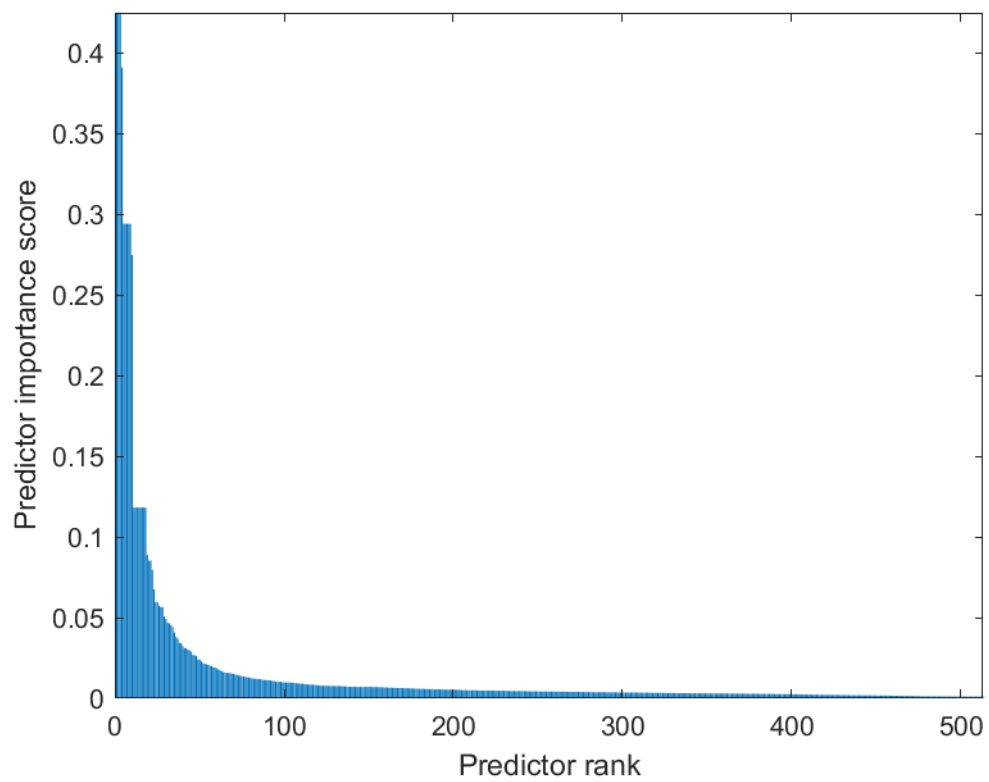


Figure S3. Scattering sub-space selection using Minimum Redundancy Maximum Relevance (MRMR) algorithm.

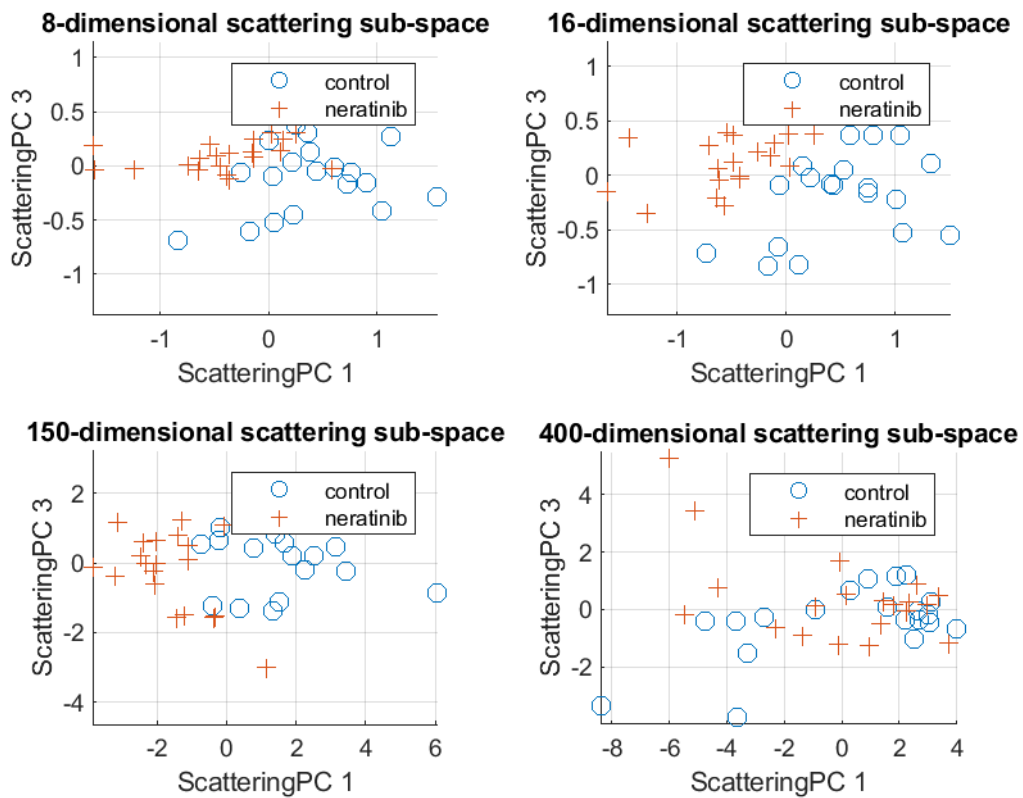


Figure S4. Scattering PCA multivariate analysis results for control cells vs neratinib-treated cells (1.0 μM concentration) at various scattering sub-space dimensions.

MTT assay

The MTT viability assay can be used to analyse cytostatic or cytotoxic drugs colorimetrically.⁴ The MTT assay was performed as shown in Figure S5 and it depends on the reduction of yellow water-soluble MTT to purple insoluble formazan crystals by mitochondrial reductase enzymes of living cells. The treated and untreated cells are compared in a dose-response curve.⁵ In these measurements, cells were treated with 0.1, 0.5, 1, 5, 20 and 50 μM of lapatinib or neratinib. The cell viability of lapatinib-treated cells is decreasing gradually and even with the highest concentration of 50 μM drug still, around 15 % of cells are alive. However, with concentrations between 0.1-5 μM lapatinib, the cell viability can be considered similar to untreated cells within the error bars. In comparison with lapatinib, neratinib seems to be more cytotoxic at lower concentrations as the cell viability is dropping with a higher concentration very strongly. This is also seen in the RTCA, where the cell index of neratinib-treated cells is decreasing after treatment with each concentration, while in cells treated with 0.1 μM lapatinib, the cell index is slowly increasing (Figure 2, red trace). The MTT validates the rather cytostatic effect of 0.1 μM lapatinib and an increased cytotoxic effect with higher lapatinib concentration. Furthermore, the MTT in combination with the RTCA demonstrates that the viability of cells treated with a low concentration of 0.1-1 μM of both drugs is very high between 80-100 % after 16 h. Therefore, concentrations of 0.1-1 μM of both drugs were used in the experiments of the present study.

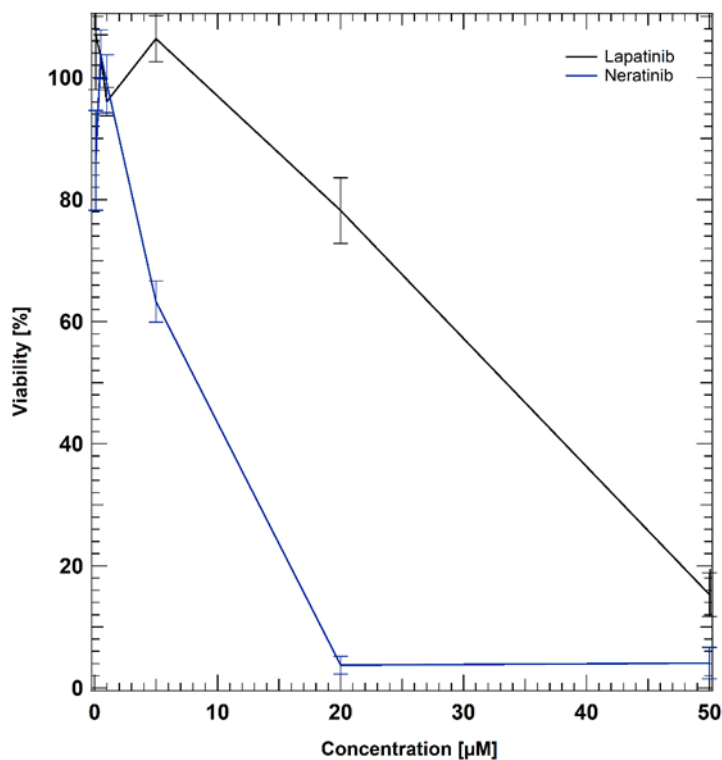


Figure S5. Dose-response curve of the MTT assay of SK-BR-3 cells, treated with lapatinib and neratinib. The graph displays the concentration in [μM] against the viability of cells in [%].

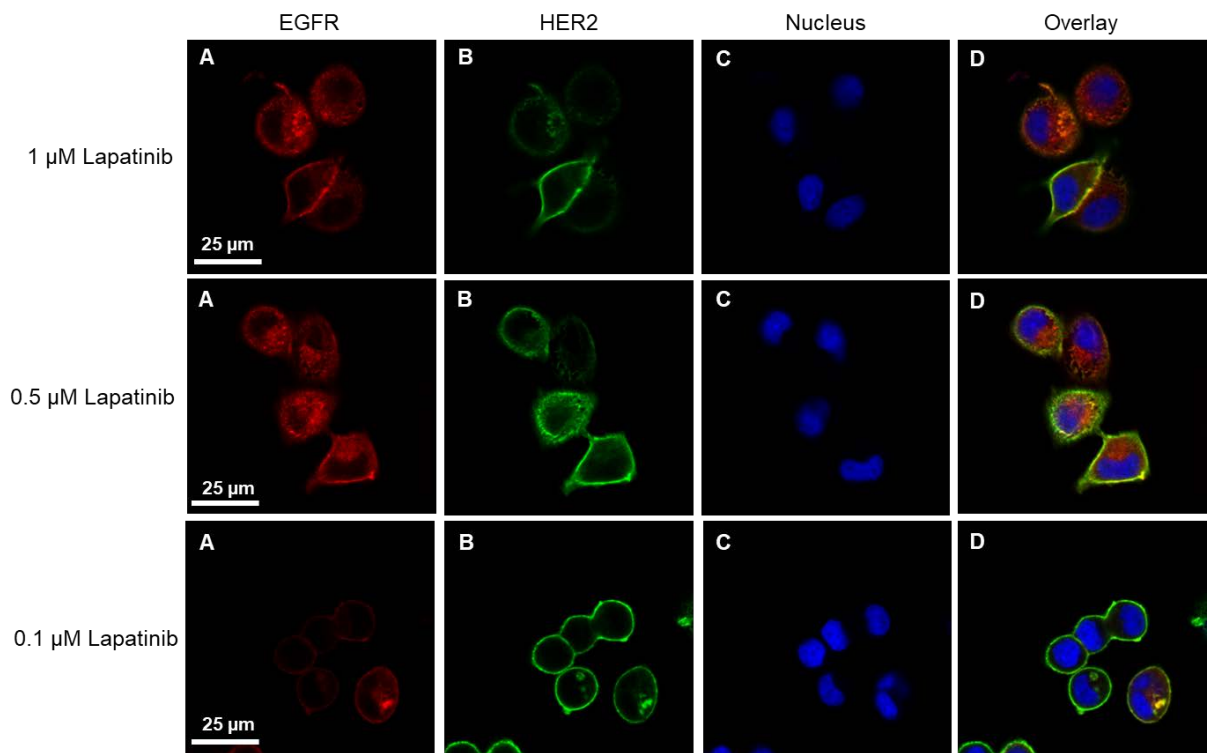


Figure S6. Fluorescence of SK-BR-3 cells treated with different lapatinib concentrations. SK-BR-3 cells stained with EGFR (red), HER2 (green) and nucleus (blue).

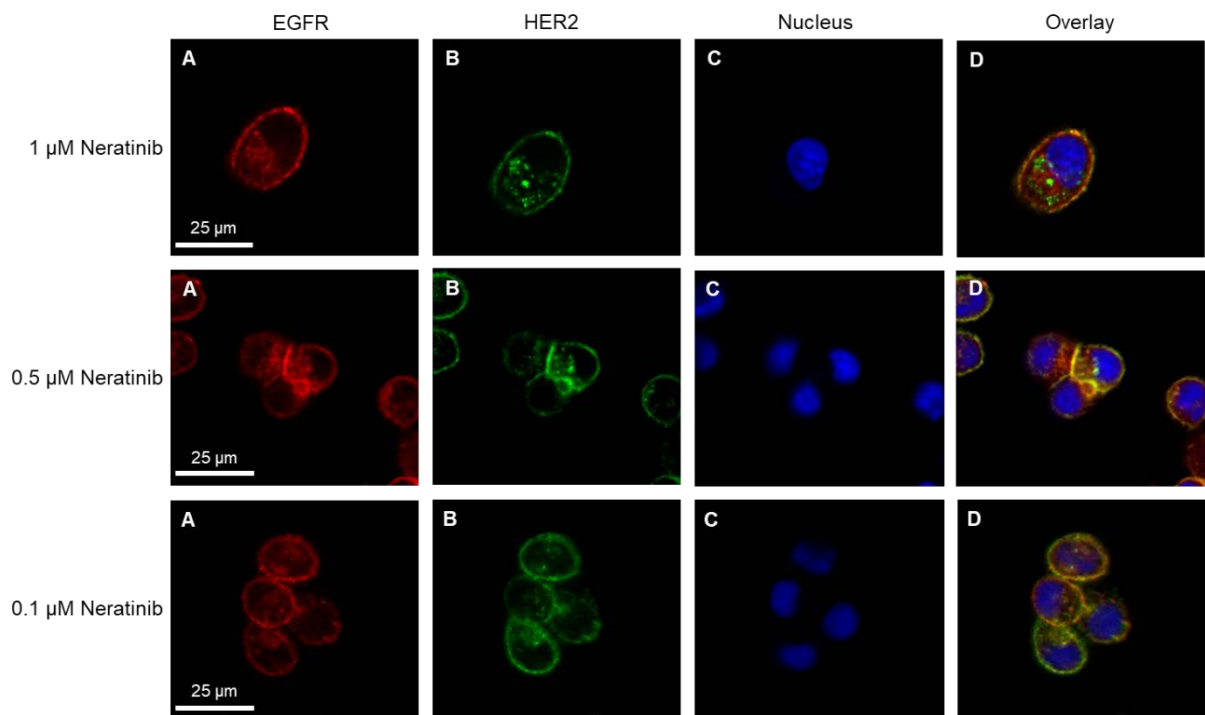


Figure S7. Fluorescence of SK-BR-3 cells treated with different neratinib concentrations. SK-BR-3 cells stained with EGFR (red), HER2 (green) and nucleus (blue).

Inhibition of ERK and AKT phosphorylation by lapatinib and neratinib

To investigate if the internalization of the receptor after drug treatment leads to any changes in the signal pathway, a Western blot was performed. It is an *in vitro* assay that is commonly used to evaluate the potency and efficacy of drug candidates by monitoring individual proteins marked by antibodies and single signal transduction pathways. In the case of TKIs targeting EGFR and HER2, it is usually used to assess the phosphorylation of downstream signalling pathways of EGFR. For instance, protein kinase B (AKT) is activated by the EGFR-activated PI-3K/AKT pathway.⁶ In addition, the extracellular-signal-regulated kinases (ERK) is the last protein in the MAP-Kinase pathway, and it is also called Ras-pathway.⁷ Erk and Akt pathways are essential for cell proliferation, cell growth, apoptosis, and cell cycle regulation, which are up-regulated in HER2-positive breast cancer.^{8,9} These proteins were stained with specific antibodies. For instance, the antibodies p-Akt, t-Akt, p-Erk 1/2, t-Erk 1/2, and β -actin were used, and the results are displayed in Figure S8. SK-BR-3 cells showed ERK (p-Erk) and Akt (p-Akt) phosphorylation when cells were not treated with lapatinib or neratinib (control). The results also indicate that the activation level of p-Erk and p-Akt is increased in cells treated with EGF compared to the control cells. This can be explained in terms of EGFR activation-induced MAP kinase activation. Besides, the signals of p-Erk and p-Akt are inhibited in the case of cells treated with different concentrations (0.1-1.0 μ M) of lapatinib or neratinib because of EGFR inhibition. Therefore, the growth and proliferation of SK-BR-3 cells were inhibited by the used drug concentrations as shown by both RTCA (Figure 2) and Western blot results (Figure S8).

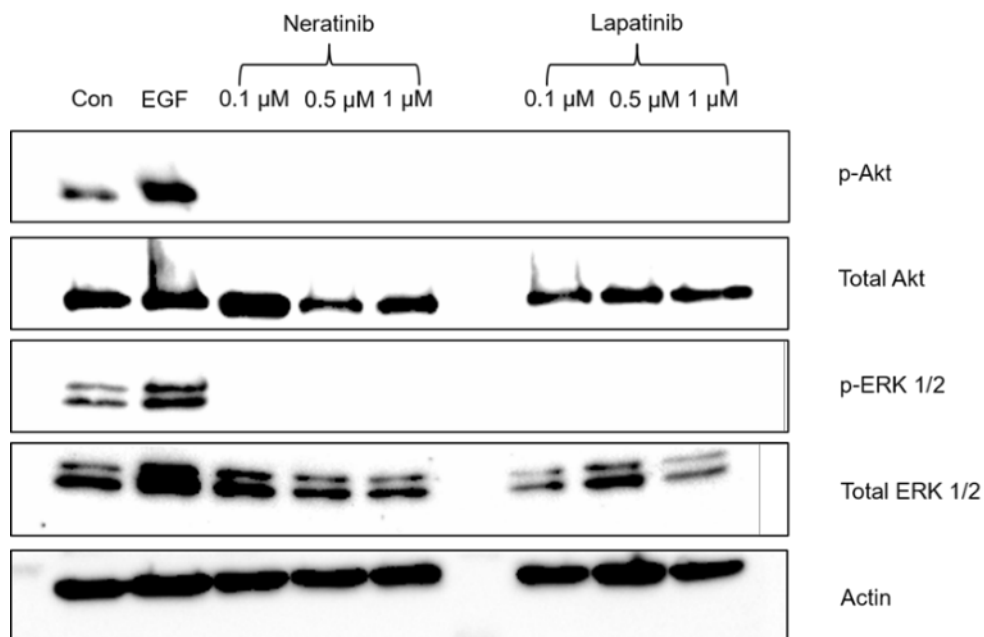


Figure S8. The Western Blot displays the effect of neratinib or lapatinib in different concentrations in comparison to untreated cells. It demonstrates the effect of the drugs on phosphorylated and dephosphorylated AKT and ERK, which occur in prominent signal pathways of cells regulating cellular proliferation and growth.

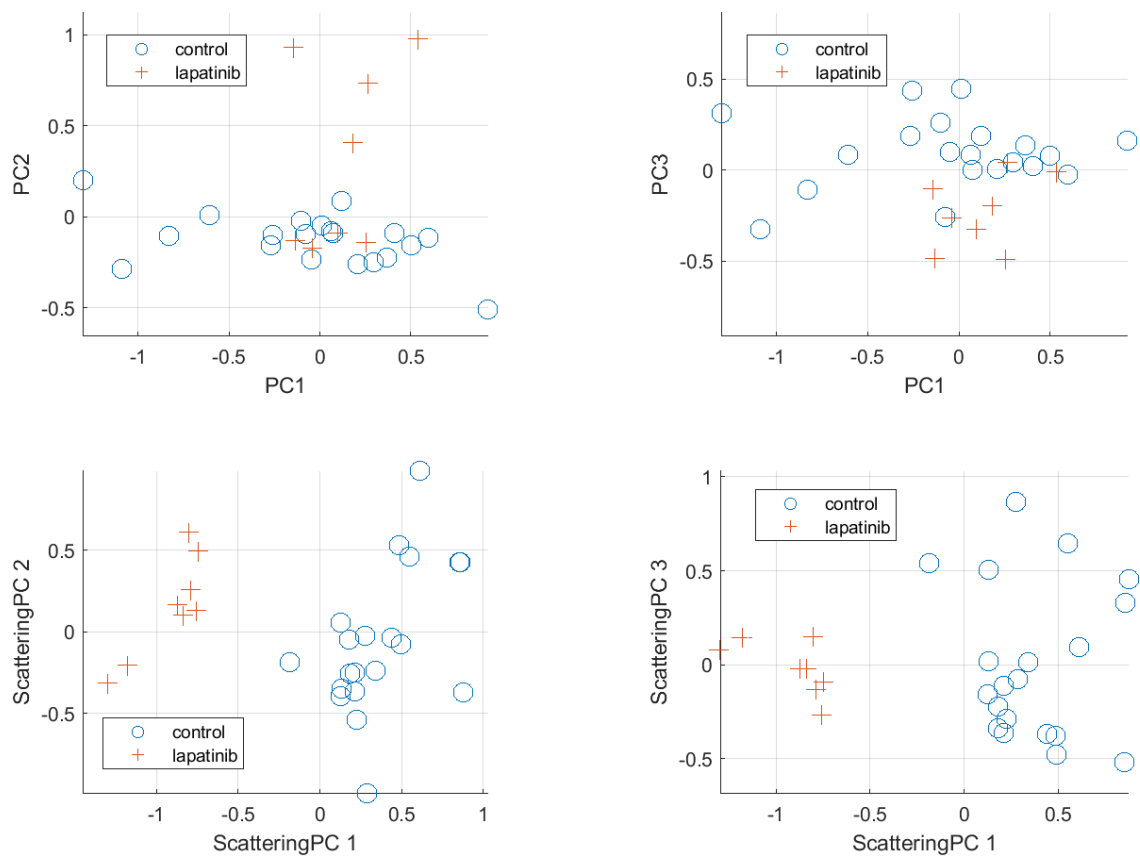


Figure S9. Scattering PCA multivariate analysis results for control cells and lapatinib-treated cells 1.0 μM concentration. Top row: principal components (PC) using standard PCA-based analysis. Bottom row: scattering principal components using proposed analysis framework.

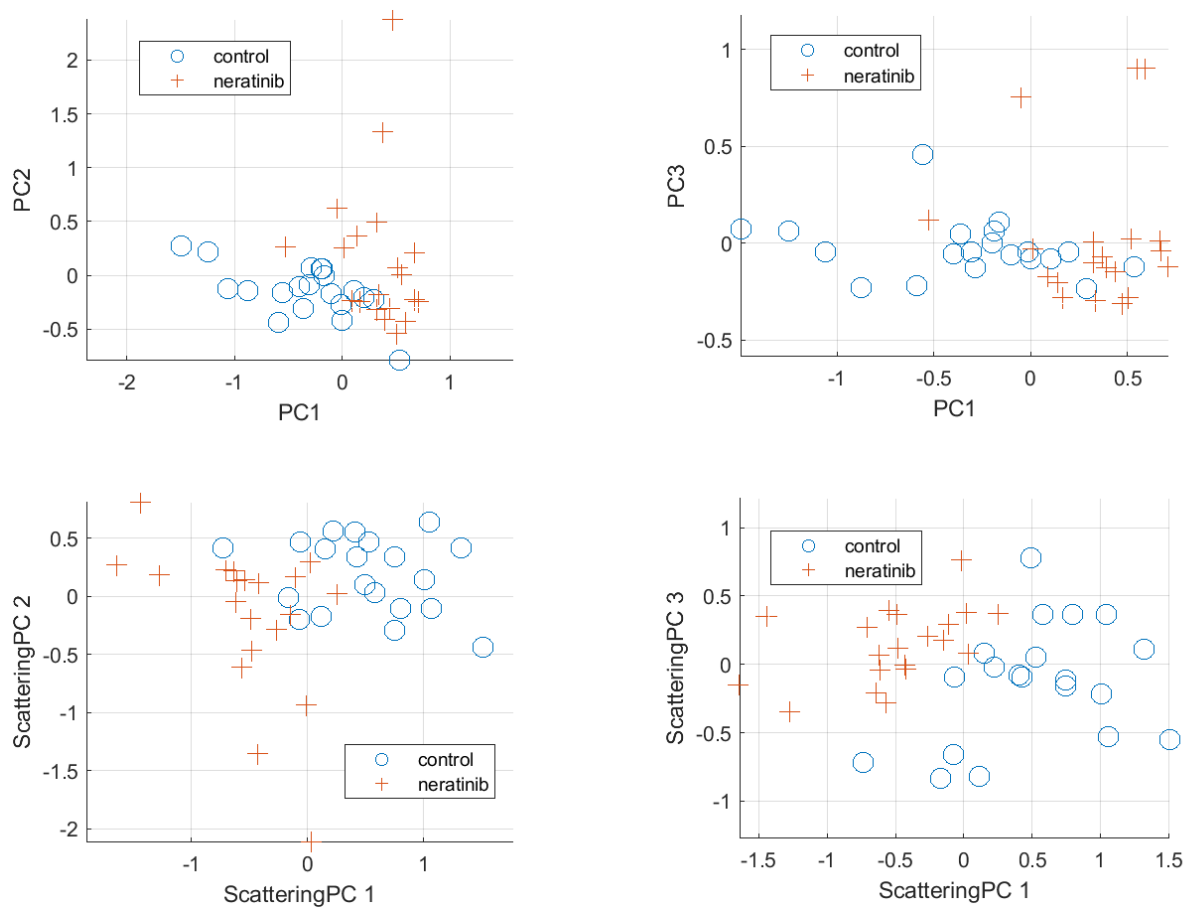


Figure S10. Scattering PCA multivariate analysis results for control cells and neratinib-treated cells 1.0 μ M concentration. Top row: principal components (PC) using standard PCA-based analysis. Bottom row: scattering Principal components using proposed analysis framework.

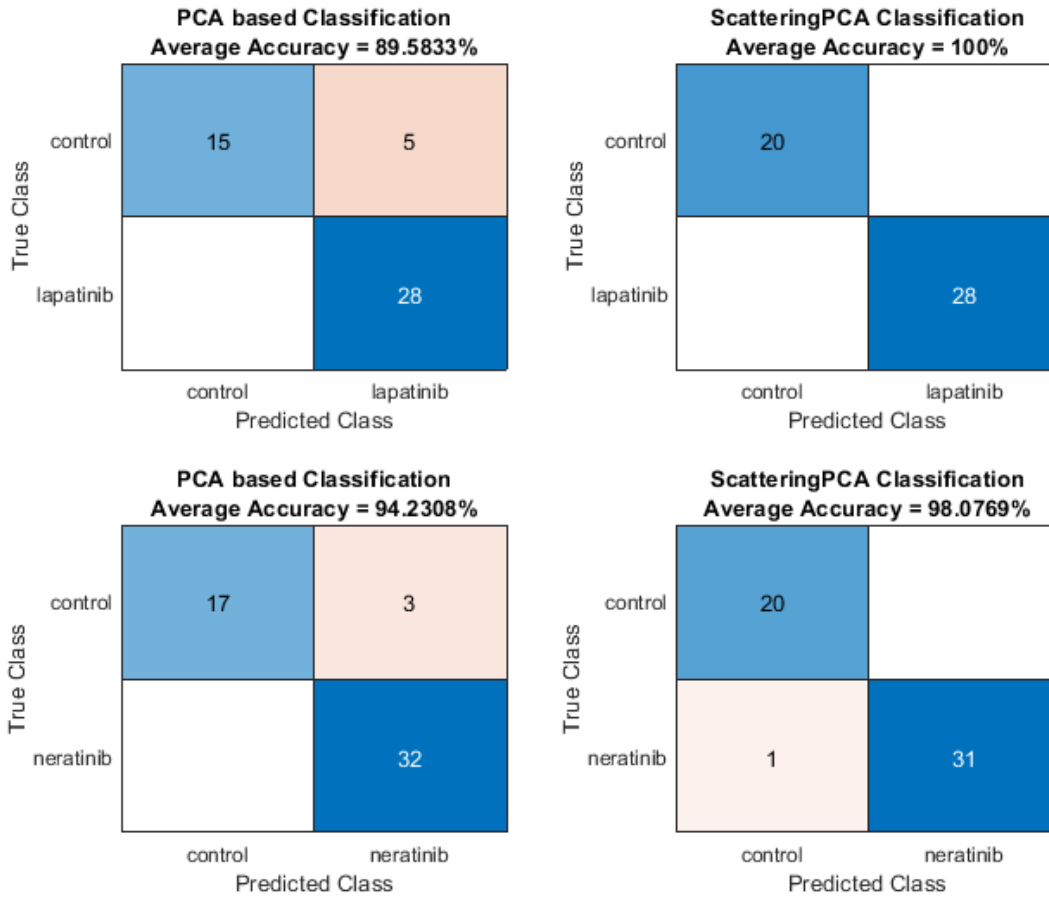


Figure S11. Confusion matrices for PCA-based classification vs proposed Scattering PCA-based classification for drug-treated cells with 0.5 μM concentrations. Top row: control vs lapatinib-treated drug cells (0.5 μM). Bottom row: control vs neratinib-treated cells (0.5 μM). A control cell is a negative case and drug-treated cell is a positive case for the classifier.



Figure S12. Confusion matrices for PCA-based classification vs proposed Scattering PCA-based classification for drug-treated cells with 1 μM concentrations. Top row: control vs lapatinib-treated drug cells (1.0 μM). Bottom row: control vs neratinib-treated cells (1.0 μM). A control cell is a negative case and drug-treated cell is a positive case for the classifier.

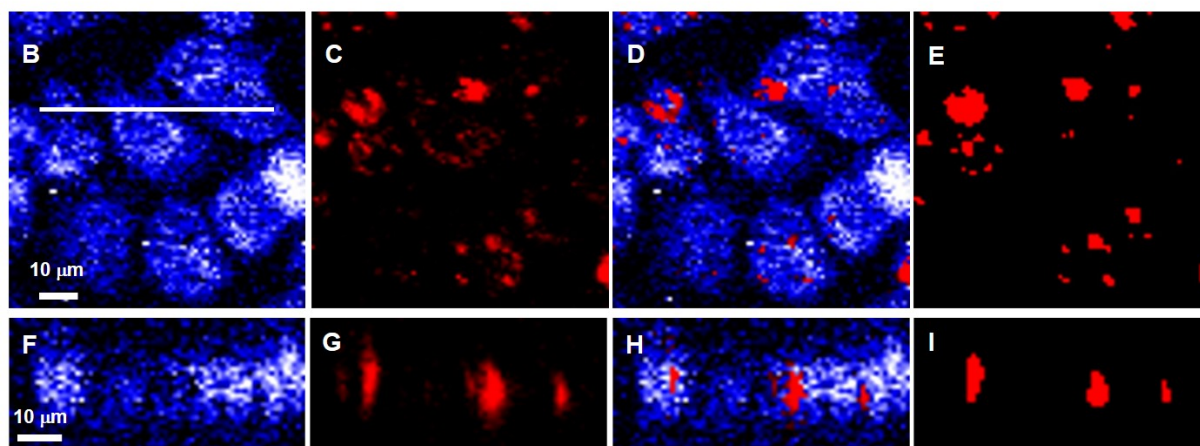
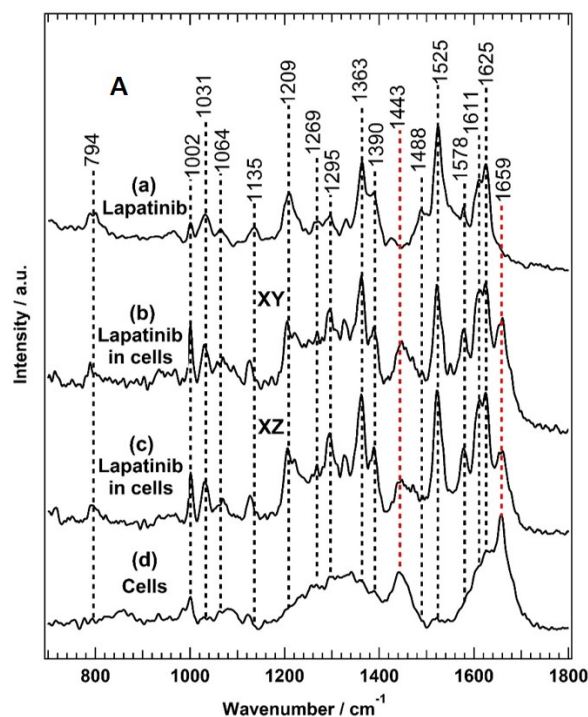


Figure S13. (A) The Raman spectra of free lapatinib (a), the average Raman spectrum of the lapatinib-containing cluster in SK-BR-3 cells shown in Panel (E) (b), the average Raman spectrum of the lapatinib-containing cluster in SK-BR-3 cells shown in Panel (I), and the average Raman spectrum of the control cells (d). (B-I) Raman imaging of SK-BR-3 cells treated with 10 μ M lapatinib for 4h. Raman images reconstructed from the band's intensities at 1420-1470 cm^{-1} (B) and 1515-1535 cm^{-1} (C). (D) Overlay of Panels B and C. (F-H) Cross-section Raman images along the x-z axis of the same cells. Scanning positions are indicated by the white line in Panel B. (E,I) represent the distribution of lapatinib (red structure) in cells. (E,I) Lapatinib-containing cluster obtained by K-means based on the Raman data shown in Panels B and F.

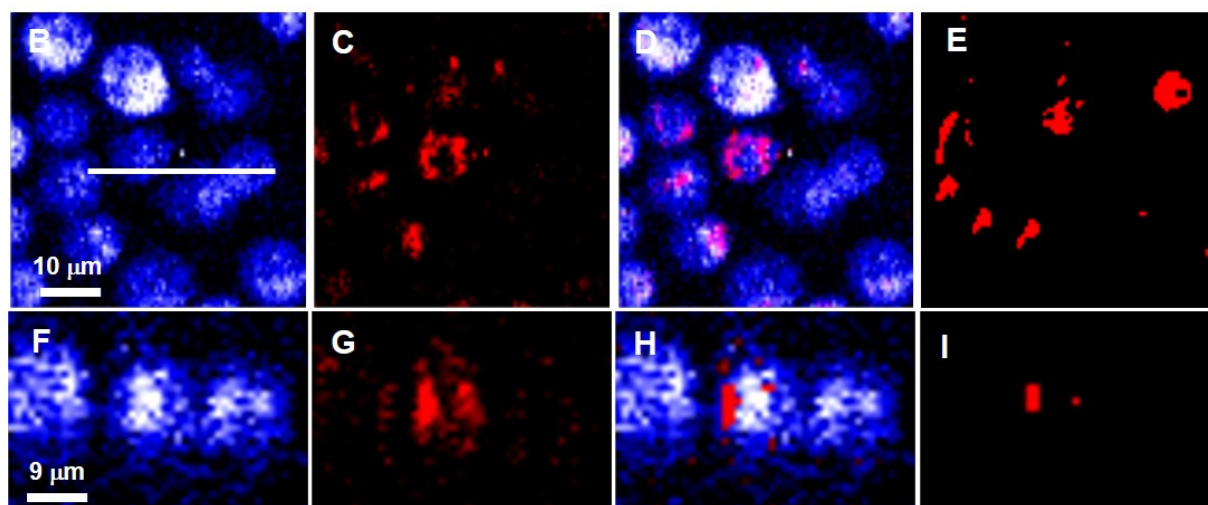
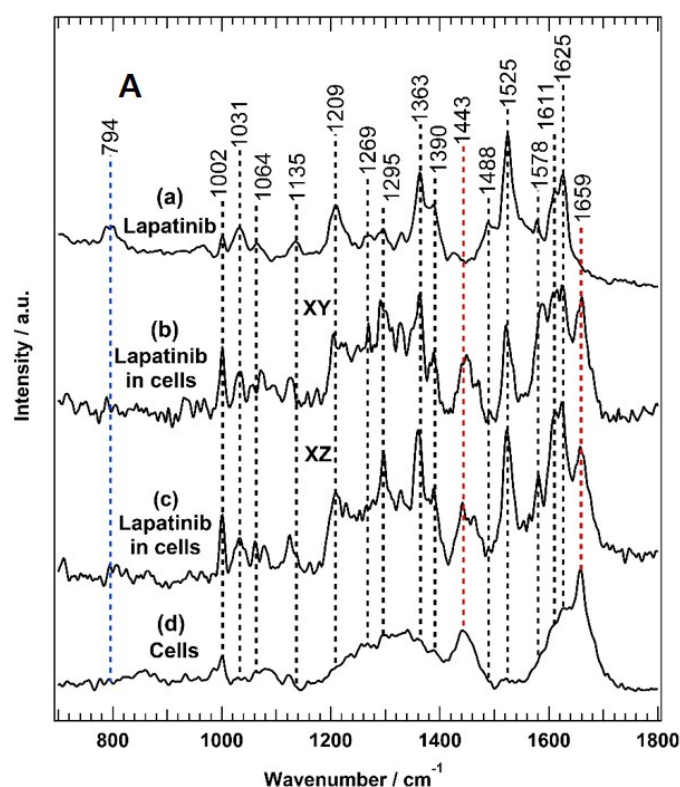


Figure S14. (A) The Raman spectra of free lapatinib (a), the average Raman spectrum of the lapatinib-containing cluster in SK-BR-3 cells shown in Panel (E) (b), the average Raman spectrum of the lapatinib-containing cluster in SK-BR-3 cells shown in Panel (I), and the average Raman spectrum of the control cells (d). (B-I) Raman imaging of SK-BR-3 cells treated with 10 μM lapatinib for 4h. Raman images reconstructed from the band's intensities at 1420-1470 cm^{-1} (B) and 1515-1535 cm^{-1} (C). (D) Overlay of Panels B and C. (F-H) Cross-section Raman images along the x-z axis of the same cells. Scanning positions are indicated by the white line in Panel B. (E,I) represent the distribution of lapatinib (red structure) in cells. (E,I) Lapatinib-containing cluster obtained by K-means based on the Raman data shown in Panels B and F.

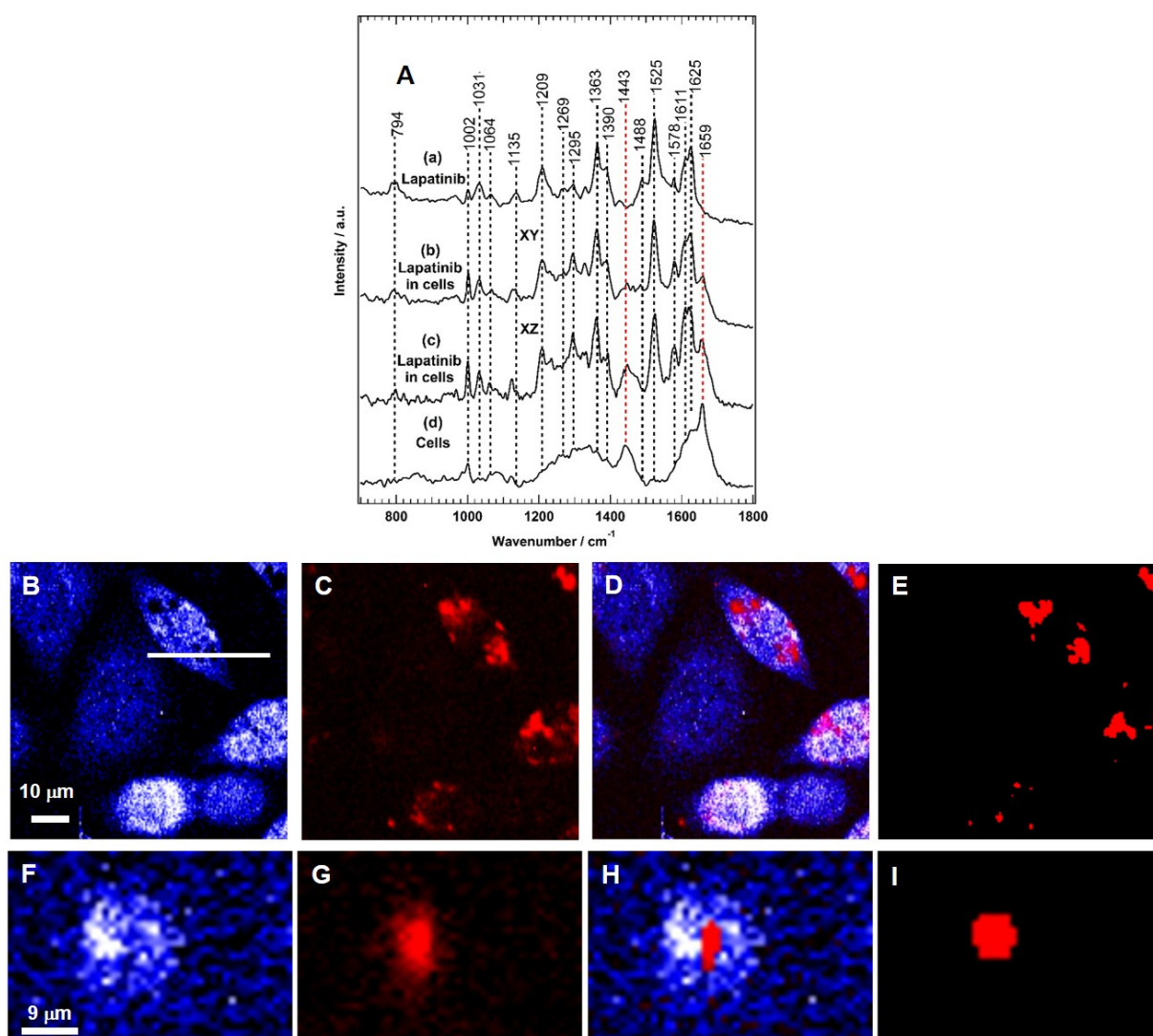


Figure S15. (A) The Raman spectra of free lapatinib (a), the average Raman spectrum of the lapatinib-containing cluster in SK-BR-3 cells shown in Panel (E) (b), the average Raman spectrum of the lapatinib-containing cluster in SK-BR-3 cells shown in Panel (I), and the average Raman spectrum of the control cells (d). (B-I) Raman imaging of SK-BR-3 cells treated with 10 μM lapatinib for 4h. Raman images reconstructed from the band's intensities at 1420-1470 cm^{-1} (B) and 1515-1535 cm^{-1} (C). (D) Overlay of Panels B and C. (F-H) Cross-section Raman images along the x-z axis of the same cells. Scanning positions are indicated by the white line in Panel B. (E,I) represent the distribution of lapatinib (red structure) in cells. (E,I) Lapatinib-containing cluster obtained by K-means based on the Raman data shown in Panels B and F.

References

- (1) *Propidium Iodide - DE*. <https://www.thermofisher.com/de/de/home/life-science/cell-analysis/fluorophores/propidium-iodide.html> (accessed 2019-10-12).
- (2) Boersma, H. H.; Kietselaer, B. L. J. H.; Stolk, L. M. L.; Bennaghmouch, A.; Hofstra, L.; Narula, J.; Heidendal, G. A. K.; Reutelingsperger, C. P. M. Past, Present, and Future of Annexin A5: From Protein Discovery to Clinical Applications*. *J. Nucl. Med.* **2005**, *46* (12), 2035–2050.
- (3) Barbash, O.; Alan Diehl, J. Chapter 13 - Regulation of the Cell Cycle. In *The Molecular Basis of Cancer (Third Edition)*; Mendelsohn, J., Howley, P. M., Israel, M. A., Gray, J. W., Thompson, C. B., Eds.; W.B. Saunders: Philadelphia, 2008; pp 177–188. <https://doi.org/10.1016/B978-141603703-3.10013-5>.
- (4) Chakrabarti, R.; Kundu, S.; Kumar, S.; Chakrabarti, R. Vitamin A as an Enzyme That Catalyzes the Reduction of MTT to Formazan by Vitamin C. *J. Cell. Biochem.* **2000**, *80* (1), 133–138.
- (5) Patravale, V.; Dandekar, P.; Jain, R. 4 - Nanotoxicology: Evaluating Toxicity Potential of Drug-Nanoparticles. In *Nanoparticulate Drug Delivery*; Patravale, V., Dandekar, P., Jain, R., Eds.; Woodhead Publishing Series in Biomedicine; Woodhead Publishing, 2012; pp 123–155. <https://doi.org/10.1533/9781908818195.123>.
- (6) Hemmings, B. A.; Restuccia, D. F. PI3K-PKB/Akt Pathway. *Cold Spring Harb. Perspect. Biol.* **2012**, *4* (9), a011189. <https://doi.org/10.1101/cshperspect.a011189>.
- (7) Santarpia, L.; Lippman, S. M.; El-Naggar, A. K. Targeting the MAPK–RAS–RAF Signaling Pathway in Cancer Therapy. *Expert Opin. Ther. Targets* **2012**, *16* (1), 103–119. <https://doi.org/10.1517/14728222.2011.645805>.
- (8) Ross, J. S.; Fletcher, J. A. The HER-2/Neu Oncogene in Breast Cancer: Prognostic Factor, Predictive Factor, and Target for Therapy. *The Oncologist* **1998**, *3* (4), 237–252.
- (9) Hasmann. Chapter 9 - Targeting HER2 by Monoclonal Antibodies for Cancer Therapy. In *Introduction to Biological and Small Molecule Drug Research and Development*; Ganellin, R., Roberts, S., Jefferis, R., Eds.; Elsevier: Oxford, 2013; pp 283–305. <https://doi.org/10.1016/B978-0-12-397176-0.00009-1>.